Workshop on Few-Body Problems in Nuclear and Hadron Physics @ITP-CAS

# Bound and Resonant Spectra of Few-Lepton Coulomb Systems

**Liang-Zhen Wen (温梁臻)**

*Center of High Energy Physics, Peking University*

Based on Phys. Rev. A 113, 032815 (2026); arxiv:2608.21901.

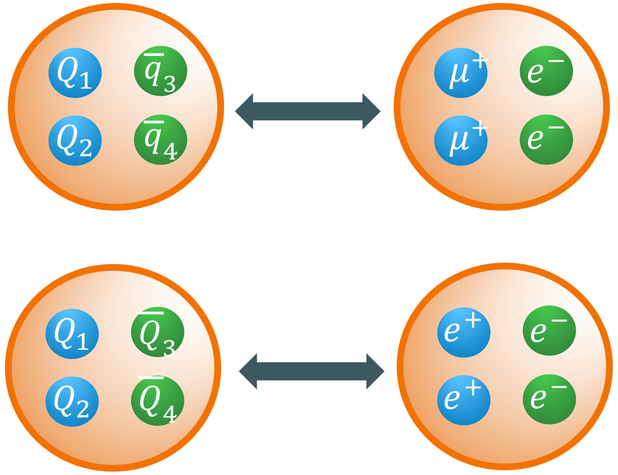
**Together with Yao Ma (TUM), Zhi-He Shen (PKU), and Shi-Lin Zhu (PKU)**

**Sep. 24, 2026, Beijing**

# Outline

- Motivation and system
- Unified theoretical framework
- Mass hierarchy and channel mixing
- Universal threshold dynamics in three-body systems
- Exchange symmetry in four-body systems

# Introduction




- Few-lepton systems as controlled QED analogues of tetraquark systems
  - Doubly heavy tetraquark $QQ\bar{q}\bar{q}$ ⟷ $\mu^+\mu^+e^-e^-$
  - Fully heavy tetraquark $QQ\bar{Q}\bar{Q}$ ⟷ $e^-e^-e^+e^+, \mu^-\mu^-\mu^+\mu^+$
- The muon introduces a strong mass hierarchy ( $m_\mu \sim 207 m_e$ )
  - Compact muonic atoms with enhanced sensitivity to nuclear size and vacuum polarization

    Pohl et al., Nature (2010); Jentschura, Ann. Phys. (2011).
  - Resonant formation of $dt\mu^-, dd\mu^-$ molecules enables muon-catalyzed fusion (μCF) Vesman, JETP Lett. (1967)

$$t\mu + D_2 \longrightarrow [(dt\mu)dee]^*, \qquad dt\mu \longrightarrow {}^4\mathrm{He} + n + \mu^- + 17.6\,\mathrm{MeV}$$

- Precisely known Coulomb dynamics
  - Provides clean benchmarks for few-body methods ( GEM, SVM, …)

# Experimental progress

- Bound-state milestones
  - Observation of $Ps^-$ ($e^-e^-e^+$) via Doppler-shifted annihilation γ rays Mills, PRL (1981)
  - Observation of $Mu^-(e^-e^-\mu^+)$ in vacuum via moderator emission and beam-foil electron capture

    Harshman et al., PRL (1986); Kuang et al., PRA (1987, 1989)
  - Observation of $Ps_2$ ($e^-e^-e^+e^+$) formation via time-resolved annihilation γ rays Cassidy & Mills, Nature (2007)
  - Observation of the $Ps_2$ ($e^-e^-e^+e^+$) L=1 excited state via laser excitation and subsequent photoionization

    Cassidy et al., PRL (2012)
- Resonant-state milestones
  - Observation of the $Ps^-$ ($e^-e^-e^+$) $^1P^o$ shape resonance via laser photodetachment

    Michishio et al., Nat. Commun. (2016)
  - Observation of $dd\mu^*$ resonances probed by high-resolution X-ray spectroscopy Toyama et al., Sci. Adv. (2026)

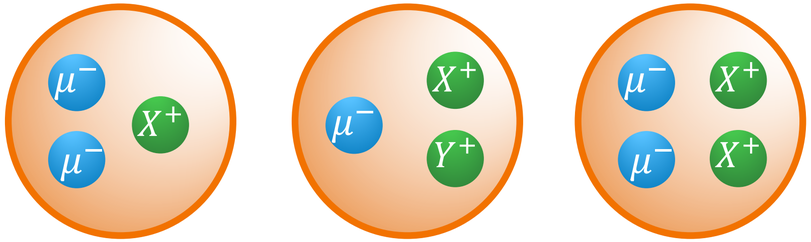
Experiments have accessed both bound-state spectra and resonances.

# Systems in this work

The systems span atomic, molecular, and equal-mass limits

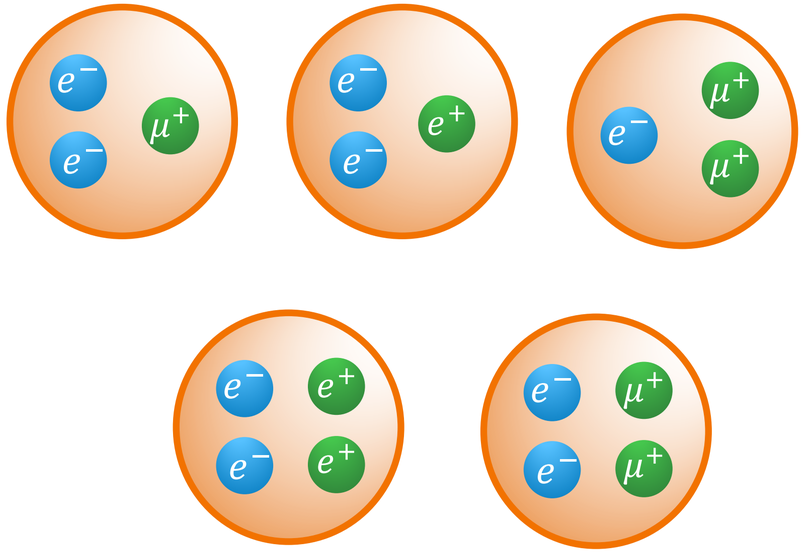
## Muon–nucleus systems

- Doubly muonic ions: $\mu^-\mu^- X^+$ $(X = p, d, t)$
- Muonic molecular ions: $\mu^- X^+ Y^+$ $(Y = p, d, t)$
- Doubly muonic molecules: $\mu^-\mu^- X^+ X^+$




## Purely leptonic systems

- trilepton ions: $e^- e^- \mu^+,\ e^- e^- e^+,\ e^- \mu^+ \mu^+$
- tetralepton molecules: $e^- e^- e^+ e^+,\ e^- e^- \mu^+ \mu^+$



# One Coulomb Hamiltonian, different thresholds

$$H = \sum_{i=1}^{N} \frac{\mathbf{p}_i^2}{2m_i} + \sum_{i<j}^{N} \alpha \frac{Q_i Q_j}{r_{ij}}, \qquad Q_i = \pm 1.$$

## Muon–nucleus atoms

| State | $E$ [eV] | $r_{\mathrm{rms}}$ [pm] |
|---|---|---|
| $p\mu(1S)$ | $-2528.49$ | 0.493 |
| $p\mu(2S)$ | $-632.12$ | 1.845 |
| $d\mu(1S)$ | $-2663.20$ | 0.468 |
| $d\mu(2S)$ | $-665.80$ | 1.752 |
| $t\mu(1S)$ | $-2711.24$ | 0.460 |
| $t\mu(2S)$ | $-677.81$ | 1.721 |

Increasing reduced mass deepens the thresholds

## Purely leptonic atoms

| State | $E$ [eV] | $r_{\mathrm{rms}}$ [nm] |
|---|---|---|
| $\mathrm{Ps}(1S)$ | $-6.8028$ | 0.183 |
| $\mathrm{Ps}(2S)$ | $-1.7007$ | 0.686 |
| $\mathrm{Ps}(2P)$ | $-1.7007$ | 0.580 |
| $\mathrm{Mu}(1S)$ | $-13.5402$ | 0.092 |
| $\mathrm{Mu}(2S)$ | $-3.3851$ | 0.345 |
| $\mathrm{Mu}(2P)$ | $-3.3851$ | 0.291 |

Degenerate $2S$–$2P$ thresholds

**These two-body levels define every dissociation threshold used below.**

# Wave function and symmetry

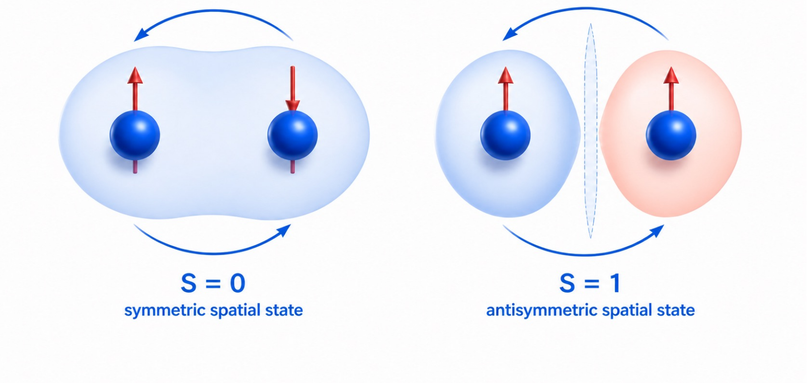
- Total wave function:

$$\Psi = \mathcal{A}(\chi_r \otimes \chi_s), \qquad \mathcal{A} : (\text{anti})\text{symmetrization of identical particles.}$$

- Pure Coulomb interaction ⇒ total orbital angular momentum L is conserved.

- Without spin-dependent forces, pair spins are good quantum numbers (e.g.,$S_{pp}$, $S_{\mu\mu}$, $S_{ee}$)
  - 3-body systems: $(S_{12}, L) \equiv {}^{2S_{12}+1}L^{\pi}$
  - 4-body systems: $(S_{12}, S_{34}, L)$

- Pair spins determine the allowed exchange symmetry of the spatial wave function $\chi(r)$
- Natural parity: $\pi = (-1)^L, \qquad L = 0,1.$



# Complex scaling method (CSM)

A method to obtain energies and wave functions of bound and resonant states.

In CSM, the coordinate $r$ and its conjugate momentum $p$ are transformed as

$$U(\theta)\boldsymbol{r} = \boldsymbol{r}e^{i\theta}, \quad U(\theta)\boldsymbol{p} = \boldsymbol{p}e^{-i\theta}$$

Avoid mistaking scattering states as resonant states

The complex-scaled Hamiltonian

$$H(\theta) = \sum_{i=1}^{4}\left(m_i + \frac{p_i^2 e^{-2i\theta}}{2m_i}\right) + \sum_{i<j=1}^{4} V_{ij}\left(r_{ij}e^{i\theta}\right)$$

no longer hermitian, has complex eigenvalues

The properties of solutions of the complex-scaled Schrödinger equation (the ABC theorem):

Bound states: not change by scaling

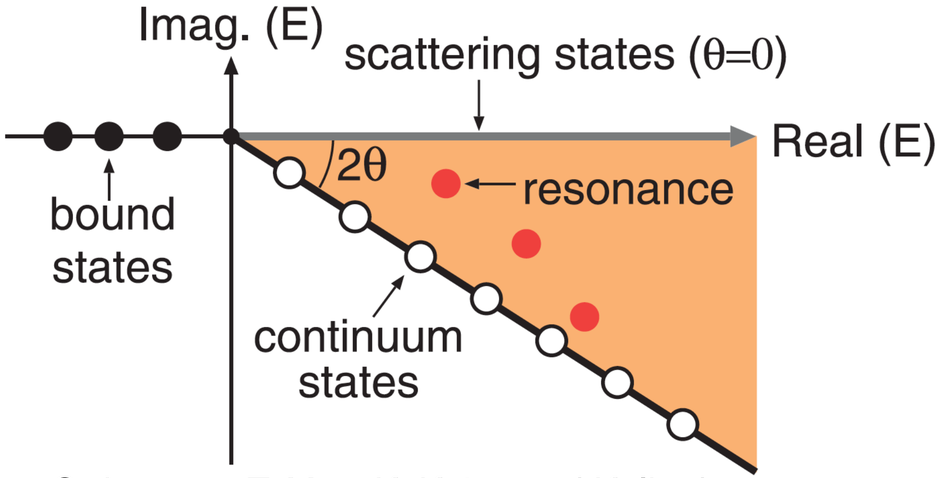
Aguilar:1971ve, Balslev:1971vb

Resonance: $E_R = M_R - i\Gamma_R/2 \xrightarrow[2\theta > |Arg(E_R)|]{\boldsymbol{r} \to \boldsymbol{r}e^{i\theta}}$ square-integrable function

Continuum states: start at the threshold, rotate clockwise by $2\theta$

CSM was advocated to derive resonances in many-body systems.

B. Simon, Communications in Mathematical Physics, 27(1): 1–9 (1972)




S. Aoyama, T. Myo, K. Kat.o, and K. Ikeda, Progress of theoretical physics 116, 1 (2006)

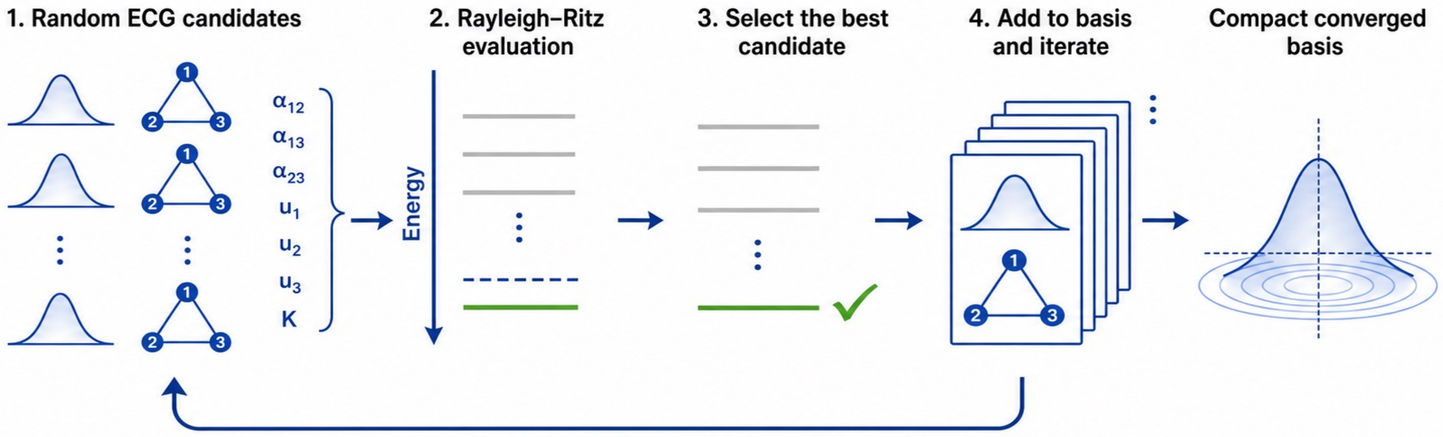
# Explicitly correlated Gaussians with the global-vector representation

- Variational ansatz: Explicitly correlated Gaussians (ECGs) Boys, Proc. R. Soc. A (1960); Singer, Proc. R. Soc. A (1960)

$$\psi(\mathbf{r}) = \underbrace{|\mathbf{v}|^{2K+L} Y_{LM}(\hat{\mathbf{v}})}_{\text{orbital motion}} \underbrace{\exp\left[-\sum_{i>j}^{N} \alpha_{ij}(\mathbf{r}_i - \mathbf{r}_j)^2\right]}_{\text{pair correlations}}, \qquad \mathbf{v} = \sum_{i=1}^{N} u_i \mathbf{r}_i.$$

$$\alpha_{ij}\text{: correlations}, \qquad u_i\text{: global} - \text{vector coefficients}, \qquad K\text{: radial flexibility}.$$

- Stochastic variational method (SVM) Varga & Suzuki, PRC (1995)




Variational optimization targets bound states

# Extended SVM: explicit cluster configurations

**Energy minimization alone does not efficiently resolve resonances**

$$\Psi_{\text{trial}} = \Psi_{\text{random}} + \Psi_{\text{molecular}}$$

$$\Psi_{\text{molecular}} = \phi_{\text{atom}}(\boldsymbol{r}_{\text{intra}})\, e^{-\boldsymbol{r}_{\text{inter}}^{\prime 2}/r_n^2}\, \theta_{LM}\left(\sum_i u_i \boldsymbol{r}_i\right), \qquad r_n = r_1 a^{n-1}$$

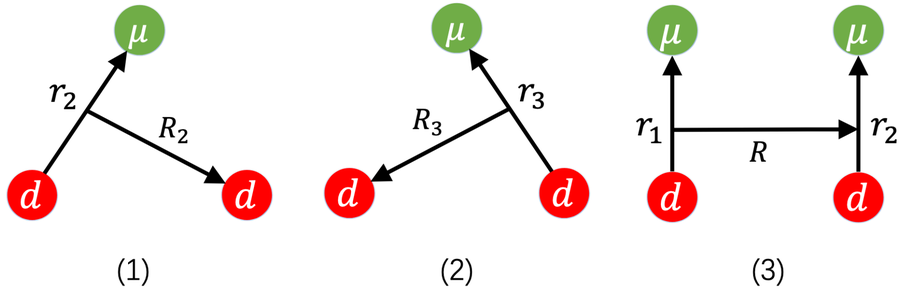


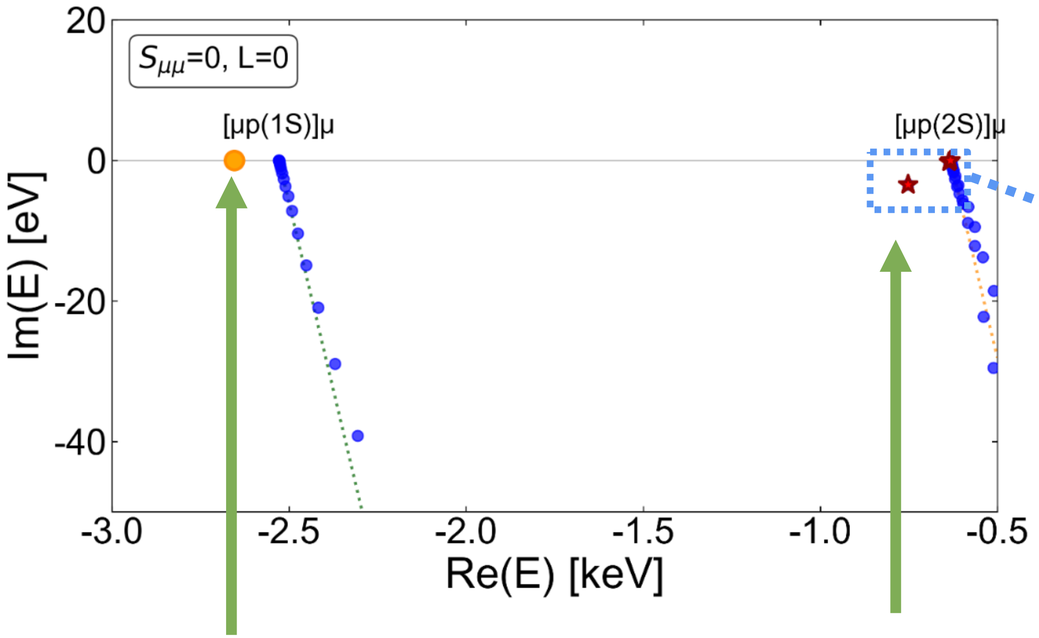

FIG. 2. Molecular configurations for the $dd\mu$ and $\mu\mu dd$ systems in extended SVM.

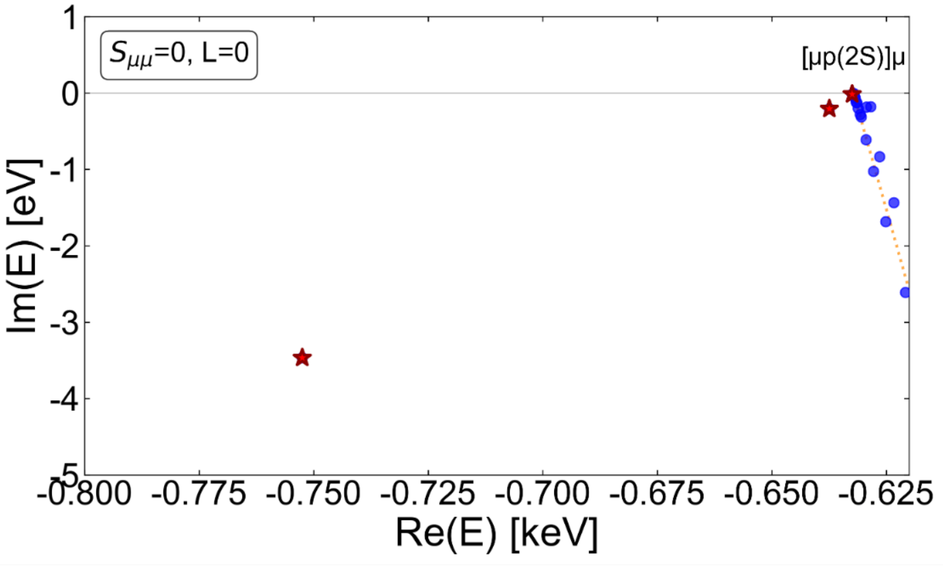
- Random ECGs describe compact and strongly correlated configurations.
- Atom–spectator and atom–atom bases describe the asymptotic cluster motion.
- Geometrically spaced intercluster Gaussians $e^{r_{inter}^2}/r_n^2$ cover short- and long-range motion.

CSM identifies the pole; ESVM supplies the basis required to stabilize it.

# $\mu^-\mu^-p$: benchmark and new near-threshold resonances

$(S_{\mu\mu}, L) = (0,0)$channel




bound state

resonant states

| system | $(S_{\mu\mu}, L)$ | $E$ [eV] | $r_{\mu\mu}^{rms}$ [pm] | $r_{\mu p}^{rms}$ [pm] | $E_{bench}$ [eV] |
|---|---|---|---|---|---|
| $\mu\mu p$ | [0,0] | -2654.93 | 1.46 | 1.02 | 2654.93 |
| | [0,0] | 752.54-3.5i | 6.8 | 4.6 | -752.60-3.6i |
| | [0,0] | -637.41-0.2i | 13.0 | 8.7 | |
| | [0,0] | -632.43 | 51.5 | 35.8 | |

$p\mu(2S)$ $-632.12$

- 1 bound state + 3 resonances (below 2nd threshold)
- Consistent with correlated–exponential calculation Liverts & Barnea, Comput. Phys. Commun. (2013)
  - $\Delta E < 0.01eV$ (bound state),
  - $\Delta(\Gamma/2) < 0.1eV$ (1st resonance)
- Additional resonances predicted by the explicit cluster basis

# Atomic three-body ions exhibit a near one-to-one spectrum

## $\mu^-\mu^-p, \mu^-\mu^-d, \mu^-\mu^-t$

| system | $(S_{\mu\mu}, L)$ | $E$ [eV] |
|---|---|---|
| $\mu\mu p$ | [0,0] | -2654.93 |
| | **p$\mu$(n = 1)** | -2528.49 |
| | [0,0] | 752.54-3.5i |
| | [0,0] | -637.41-0.2i |
| | [0,0] | -632.43 |
| | [1,0] | -642.21 |
| | [1,0] | -632.70 |
| | [0,1] | -637.22 |
| | [0,1] | -632.28 |
| | [1,1] | -720.48-0.1i |
| | [1,1] | -634.29 |
| | **p$\mu$(n = 2)** | -632.12 |
| $\mu\mu d$ | [0,0] | -2802.55 |
| | **d$\mu$(n = 1)** | -2663.20 |
| | [0,0] | -792.31-4.3i |
| | [0,0] | -671.27-0.2i |
| | [0,0] | -666.11 |
| | [1,0] | -676.66 |
| | [1,0] | -666.41 |
| | [0,1] | -671.24 |
| | [0,1] | -665.97 |
| | [1,1] | -757.82-0.2i |
| | [1,1] | -668.01 |
| | **d$\mu$(n = 2)** | -665.80 |
| $\mu\mu t$ | [0,0] | -2855.68 |
| | **t$\mu$(n = 1)** | -2711.24 |
| | [0,0] | -806.75-4.5i |
| | [0,0] | -683.35-0.2i |
| | [0,0] | -678.12 |
| | [1,0] | -688.97 |
| | [1,0] | -678.44 |
| | [0,1] | -683.39 |
| | [0,1] | -677.98 |
| | [1,1] | -771.20-0.3i |
| | [1,1] | -680.05 |
| | **t$\mu$(n = 2)** | -677.81 |

## $\mu^+e^-e^-$

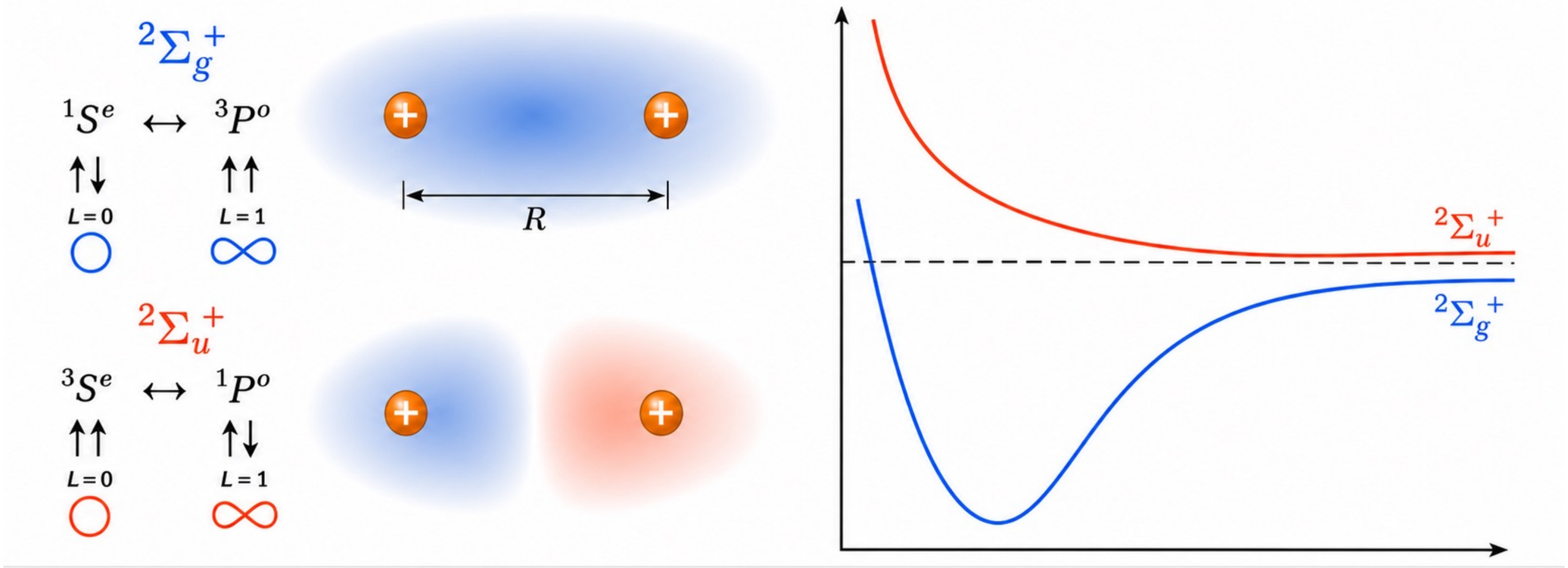
TABLE IV. Complex energies $E - i\Gamma/2$ of the $\mu^+e^-e^-$ bound and resonant states below the second threshold $\mathrm{Mu}(2) + e^-$, grouped by the quantum numbers $(S_{12}, L)$ and labeled by the term symbol $^{2S_{12}+1}L^{\pi}$. Energies are in eV and half-widths $\Gamma/2$ in meV. "B"/"R" denote bound/resonant states. An asterisk (*) marks widths that are not fully $\theta$-converged and are only qualitative estimates. In the two rightmost columns, results from the literature are presented for comparison, obtained with the correlated-exponential method [32, 33].

| | | | This work | | Lit. | |
|---|---|---|---|---|---|---|
| | $v$ | type | $E$ | $\Gamma/2$ | $E$ | $\Gamma/2$ |
| $^1S^e\ (0,0)$ | | | | | | |
| | 0 | B | $-14.2875$ | 0 | $-14.2875$ [32, 33] | 0 |
| **Mu(1) + $e^-$** | | | **$-13.5402$** | | | |
| | 0 | R | $-4.0291$ | 22.695 | $-4.0288$ [32] | 23.283 |
| | 1 | R | $-3.4127$ | 1.247 | — | — |
| | 2 | R | $-3.3863$ | 0.070* | — | — |
| $^3S^e\ (1,0)$ | | | | | | |
| | 0 | R | $-3.4419$ | 0.009 | — | — |
| | 1 | R | $-3.3881$ | 0.070* | — | — |
| $^1P^o\ (0,1)$ | | | | | | |
| | 0 | R | $-3.4134$ | 0.019 | — | — |
| | 1 | R | $-3.3856$ | 0.105* | — | — |
| $^3P^o\ (1,1)$ | | | | | | |
| | 0 | R | $-3.8493$ | 2.675 | — | — |
| | 1 | R | $-3.3962$ | 0.064 | — | — |
| **Mu(2) + $e^-$** | | | **$-3.3851$** | | | |

- 1 bound state + 9 resonances
- Near one-to-one spectral correspondence

# Exchange symmetry pairs S- and P-wave sectors on each BO curve

For two identical $\mu^+$, BO parity, heavy-pair rotation, and spin exchange parity must combine to $-1$.



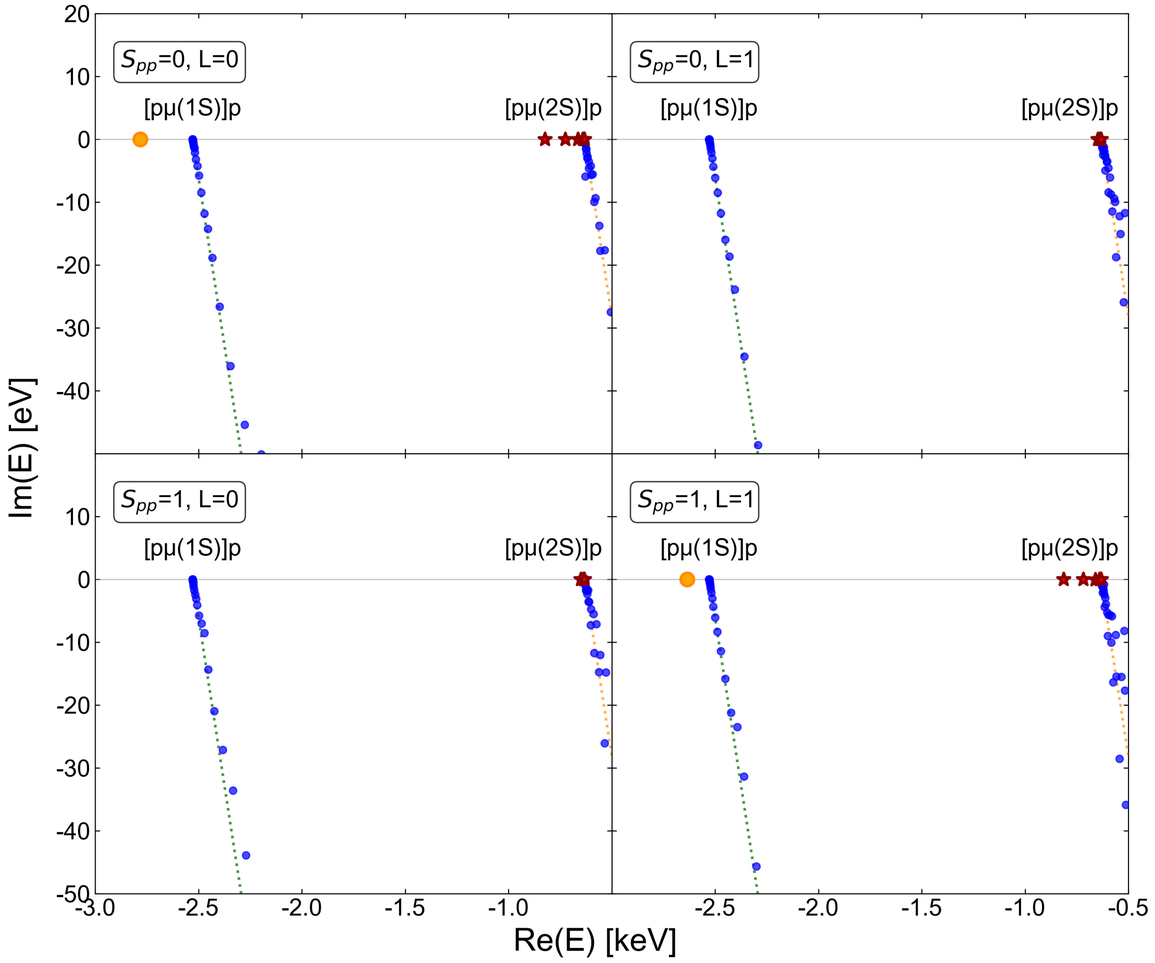

$$P_{12}\,\Psi \;=\; \eta_{\mathrm{BO}}\,(-1)^{L}\,\xi_{\mathrm{spin}}\,\Psi \;=\; -\Psi$$

$\eta_{\mathrm{BO}}$ : exchange parity of the BO electronic wave function ( $+1$ for **g**, $-1$ for **u** )

$(-1)^L$ : exchange parity of the heavy-particle rotational wave function

$\xi_{\mathrm{spin}}$ : exchange parity of the $\mu^+\mu^+$ spin wave function ( $-1$ singlet, $+1$ triplet )

# $pp\mu^-$: narrow BO-like S- and P-wave ladders




| $[S_{pp}, L]$ | $E$ [eV] |
|---|---|
| $[0,0]$ | -2781.64 |
| $[1,1]$ | -2635.76 |
| $\mathbf{p\mu(n=1)}$ | -2528.49 |
| $[0,0]$ | -823.74 |
| $[0,0]$ | -725.17 |
| $[0,0]$ | -664.08 |
| $[0,0]$ | -641.13 |
| $[0,0]$ | -634.91 |
| $[0,0]$ | -633.00 |
| $[0,0]^\dagger$ | -632.40 |
| $[1,0]$ | -649.68 |
| $[1,0]$ | -637.74 |
| $[1,0]$ | -633.90 |
| $[1,0]$ | -632.68 |
| $[1,0]$ | -632.29 |
| $[0,1]$ | -648.13 |
| $[0,1]$ | -645.69 |
| $[0,1]$ | -636.99 |
| $[0,1]$ | -633.60 |
| $[0,1]$ | -632.57 |
| $[0,1]$ | -632.24 |
| $[1,1]$ | -813.59 |
| $[1,1]$ | -717.91 |
| $[1,1]$ | -659.91 |
| $[1,1]$ | -639.67 |
| $[1,1]$ | -634.37 |
| $[1,1]$ | -632.80 |
| $[1,1]^\dagger$ | -632.30 |
| $\mathbf{p\mu(n=2)}$ | -632.12 |

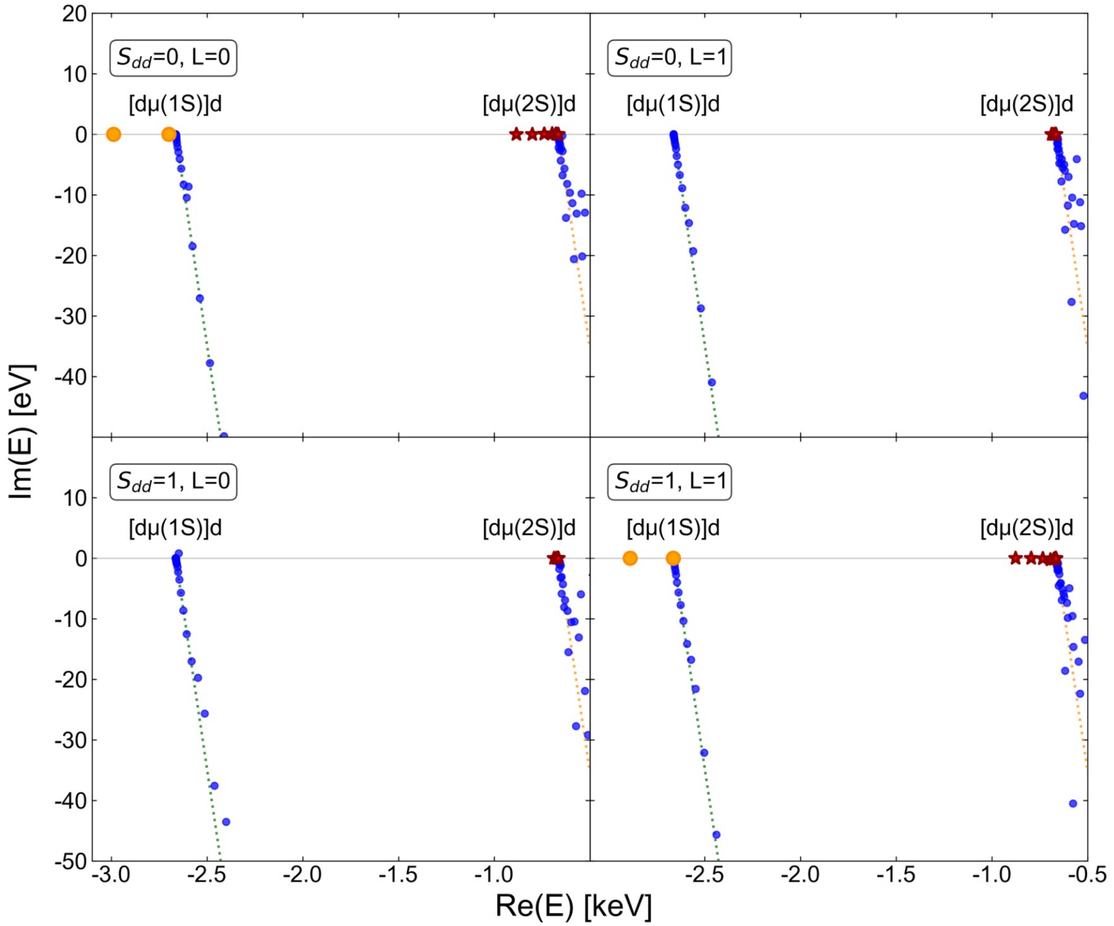
μ-H reference correction scales:

- vacuum polarization ≈205 meV
- 2S hyperfine splitting ≈23 meV
- nuclear finite-size shift ≈4 meV

Antognini et al., Ann. Phys. (2013)

- 2 bound states + 25 resonant states (including 2 newly identified shallow resonances)
- The paired S/P ladders support a BO-like organization
- Widths are below 0.1 eV (our numerical resolution)

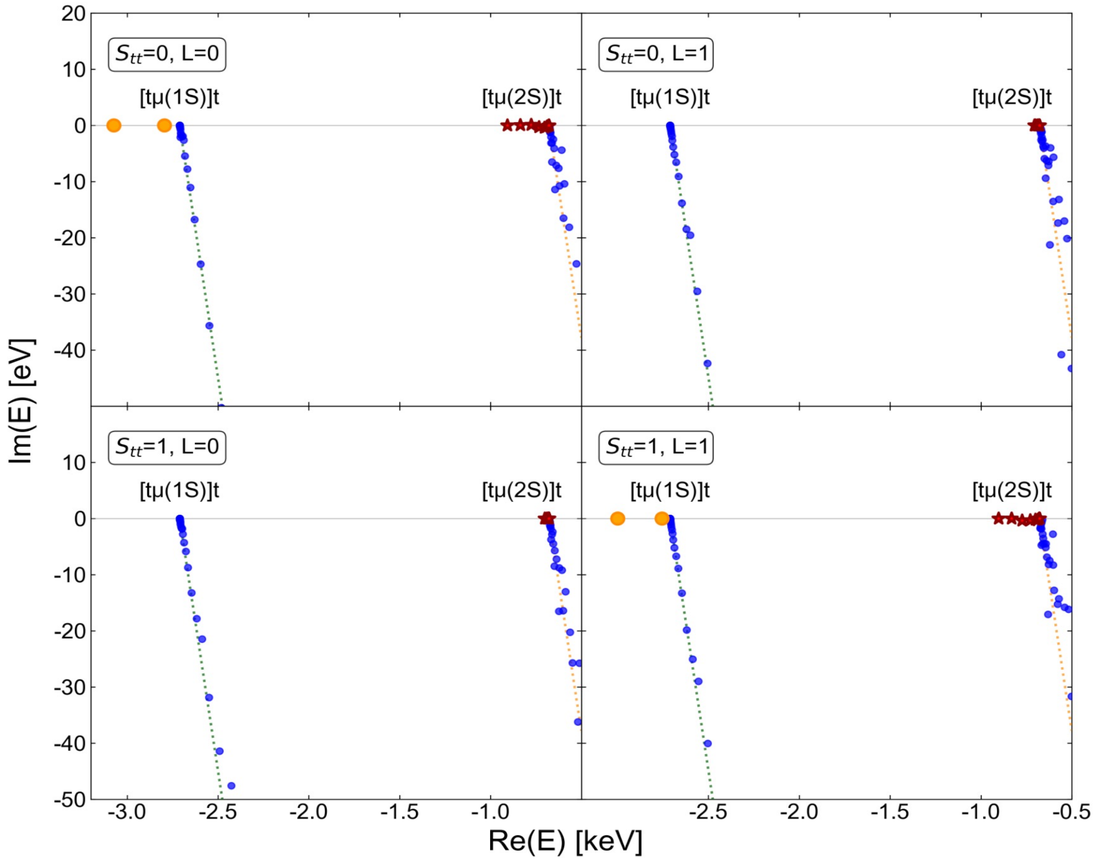
# $dd\mu^-$: increasing nuclear mass produces a denser spectrum




| $[S_{dd}, L]$ | $E$ [eV] |
|---|---|
| $[0(2), 0]$ | -2988.27 |
| $[0(2), 0]$ | -2699.04 |
| $[1, 1]$ | -2889.88 |
| $[1, 1]$ | -2665.18 |
| $\mathbf{d\mu(n = 1)}$ | -2663.20 |
| $[0(2), 0]$ | -883.91 |
| $[0(2), 0]$ | -801.08 |
| $[0(2), 0]$ | -738.76 |
| $[0(2), 0]$ | -697.59 |
| $[0(2), 0]$ | -678.32 |
| $[0(2), 0]$ | -671.06 |
| $[0(2), 0]$ | -668.05 |
| $[0(2), 0]$ | -666.76 |
| $[0(2), 0]$ | -666.21 |
| $[0(2), 0]^\dagger$ | -665.96 |
| $[1, 0]$ | -686.96 |
| $[1, 0]$ | -675.21 |
| $[1, 0]$ | -669.88 |
| $[1, 0]$ | -667.56 |
| $[1, 0]$ | -666.56 |
| $[1, 0]$ | -666.12 |
| $[1, 0]^\dagger$ | -665.92 |
| $[0(2), 1]$ | -688.44 |
| $[0(2), 1]$ | -685.92 |
| $[0(2), 1]$ | -674.60 |
| $[0(2), 1]$ | -669.55 |
| $[0(2), 1]$ | -667.39 |
| $[0(2), 1]$ | -666.47 |
| $[0(2), 1]$ | -666.04 |
| $[1, 1]$ | -877.70 |
| $[1, 1]$ | -795.98 |
| $[1, 1]$ | -734.51 |
| $[1, 1]$ | -694.78 |
| $[1, 1]$ | -677.07 |
| $[1, 1]$ | -670.47 |
| $[1, 1]$ | -667.76 |
| $[1, 1]$ | -666.62 |
| $[1, 1]$ | -666.09 |
| $[1, 1]^\dagger$ | -665.90 |
| $\mathbf{d\mu(n = 2)}$ | -665.80 |

- 4 bound states
- 34 resonant states ( including 3 newly identified states)
- The near-threshold spacing is smaller than in $pp\mu$

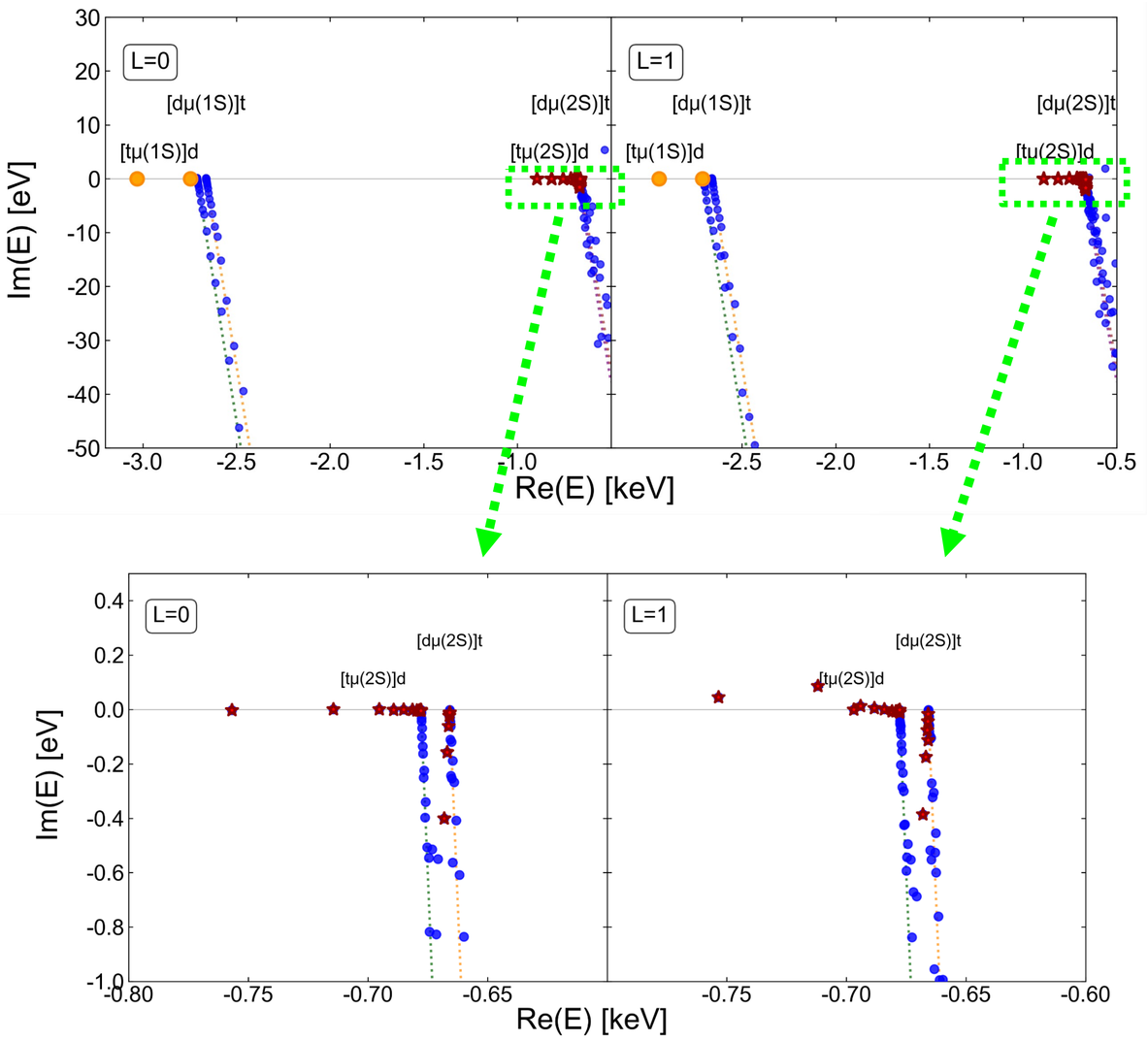
# $tt\mu^-$: the near-threshold ladder is compressed further




| $[S_{tt}, L]$ | $E$ [eV] |
|---|---|
| $[0,0]$ | -3074.1 |
| $[0,0]$ | -2795.0 |
| $[1,1]$ | -3000.4 |
| $[1,1]$ | -2756.4 |
| $\mathbf{t\mu(n=1)}$ | -2711.24 |
| $[0,0]$ | -907.94 |
| $[0,0]$ | -835.37 |
| $[0,0]$ | -776.83 |
| $[0,0]$ | -732.33 |
| $[0,0]$ | -703.81 |
| $[0,0]$ | -689.92 |
| $[0,0]$ | -683.70 |
| $[0,0]$ | -680.71 |
| $[0,0]$ | -679.24 |
| $[0,0]$ | -678.52 |
| $[0,0]$ | -678.17 |
| $[0,0]$ | -677.95 |
| $[1,0]$ | -700.74 |
| $[1,0]$ | -689.70 |
| $[1,0]$ | -683.78 |
| $[1,0]$ | -680.78 |
| $[1,0]$ | -679.29 |
| $[1,0]$ | -678.56 |
| $[1,0]$ | -678.17 |
| $[1,0]$ | -677.96 |
| $[0,1]$ | -705.24 |
| $[0,1]$ | -699.98 |
| $[0,1]$ | -689.16 |
| $[0,1]$ | -683.43 |
| $[0,1]$ | -680.55 |
| $[0,1]$ | -679.13 |
| $[0,1]$ | -678.43 |
| $[0,1]$ | -678.01 |
| $[1,1]$ | -903.45 |
| $[1,1]$ | -831.25 |
| $[1,1]$ | -773.07 |
| $[1,1]$ | -729.03 |
| $[1,1]$ | -700.85 |
| $[1,1]$ | -688.17 |
| $[1,1]$ | -682.73 |
| $[1,1]$ | -680.18 |
| $[1,1]$ | -678.93 |
| $[1,1]$ | -678.34 |
| $[1,1]$ | -677.98 |
| $\mathbf{t\mu(n=2)}$ | -677.81 |

- 4 bound states
- 39 resonant states, mostly newly reported
- The resonance sequence is denser than in $dd\mu$
- $pp\mu \rightarrow dd\mu \rightarrow tt\mu$: $larger\ nuclear\ mass \Rightarrow denser\ BO-like\ spectrum$.

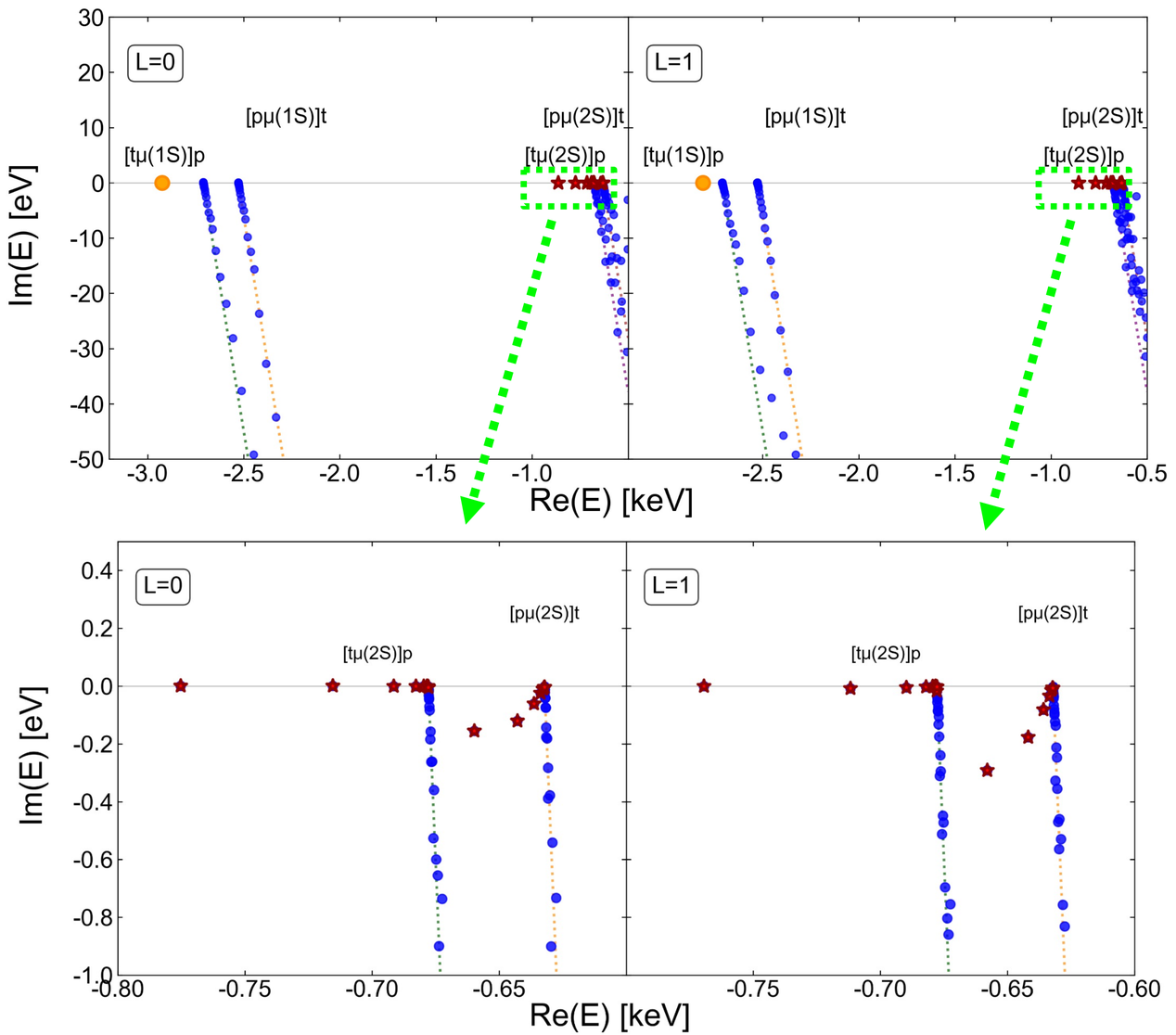
# $dt\mu^-$: near-degenerate thresholds broaden resonances




| $L$ | $E$ [eV] | $\tau$ |
|---|---|---|
| 0 | -3030.38 | |
| 0 | -2746.08 | |
| 1 | -2943.71 | |
| 1 | -2711.90 | |
| $\mathbf{t\mu(n=1)}$ | -2711.24 | |
| $\mathbf{d\mu(n=1)}$ | -2663.20 | |
| $0^\dagger$ | -678.64 | |
| $0^\dagger$ | -678.20 | |
| $1^\dagger$ | -678.52 | |
| $1^\dagger$ | -678.14 | |
| $\mathbf{t\mu(n=2)}$ | -677.81 | |
| $0^\dagger$ | -666.30 - 0.1i | |
| $0^\dagger$ | -666.03 | |
| $1^\dagger$ | -670.62 - 0.7i | |
| $1^\dagger$ | -668.03 - 0.4i | |
| $1^\dagger$ | -666.82 - 0.2i | |
| $1^\dagger$ | -666.25-0.1i | |
| $1^\dagger$ | -665.97 | |
| $\mathbf{d\mu(n=2)}$ | -665.80 | |

- 4 bound states + 33 resonances (including 11 newly reported)
- The two $n = 2$ rearrangement thresholds are close $[t\mu(n=2)]d$ and $[d\mu(n=2)]t$
- Strong channel mixing produces visibly broader poles

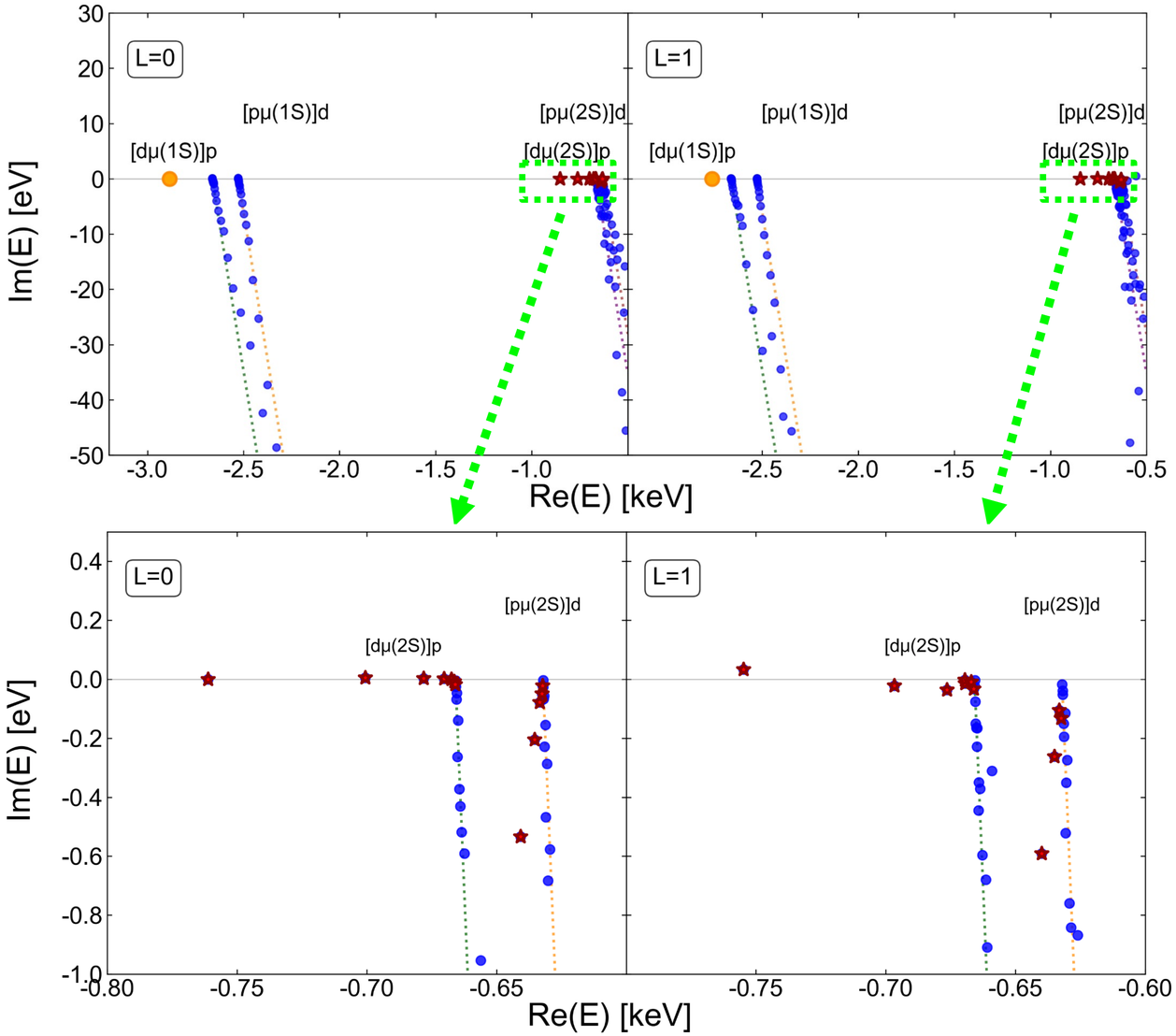
# $pt\mu^-$: wider threshold separation suppresses channel mixing




| $L$ | $E$ [eV] |
|---|---|
| 0 | -2925.08 |
| 1 | -2810.37 |
| $\mathbf{t\mu(n=1)}$ | -2711.24 |
| $\mathbf{p\mu(n=1)}$ | -2528.49 |
| ... | ... |
| $\mathbf{t\mu(n=2)}$ | -677.81 |
| 0 | -659.73 - 0.2i |
| 0 | -642.80 - 0.1i |
| 0 | -636.31 - 0.1i |
| 0 | -633.78 |
| 0 | -632.78 |
| 0 | -632.38 |
| 1 | -658.06 - 0.3i |
| 1 | -641.91 - 0.2i |
| 1 | -635.89 - 0.1i |
| 1 | -633.59 |
| 1 | -632.69 |
| 1 | -632.34 |
| $\mathbf{p\mu(n=2)}$ | -632.12 |

- 2 bound states + 29 resonances (mostly newly reported)
- The two $n = 2$ thresholds $[t\mu(n = 2)]p$ and $[p\mu(n = 2)]t$ are more widely separated than in $dt\mu^-$
- Weaker mixing produces narrower poles

# $pd\mu^-$: the wave function evolves between rearrangement channels



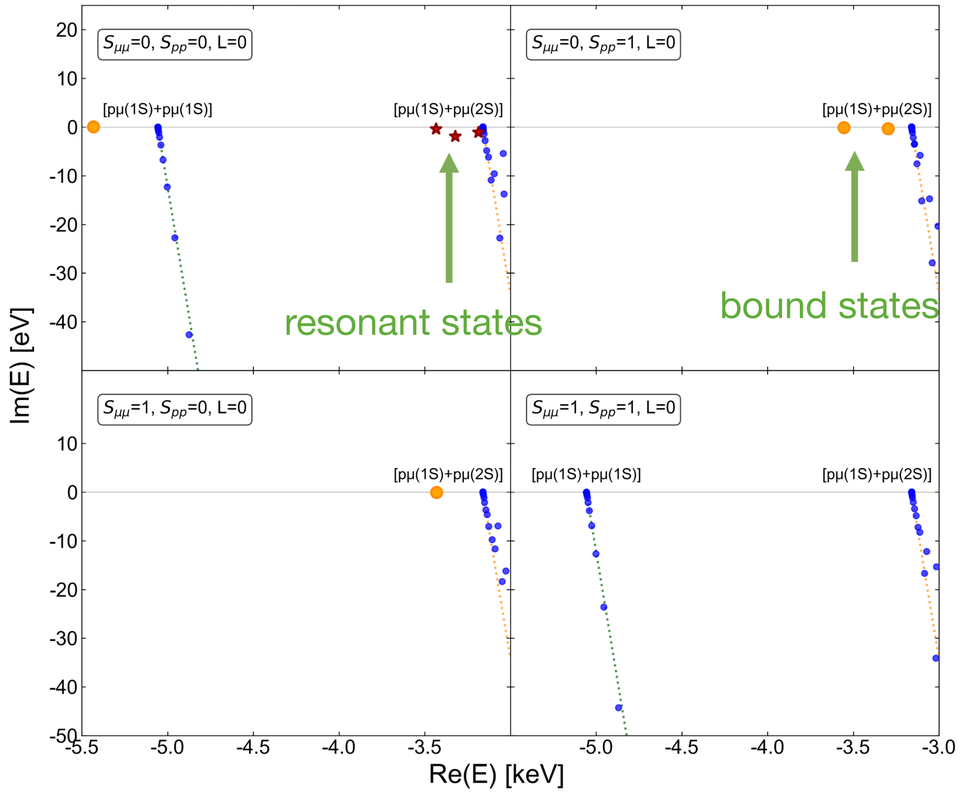

| $L$ | $E$ [eV] | $r_{pd}^{rms}$ [pm] | $r_{p\mu}^{rms}$ [pm] | $r_{d\mu}^{rms}$ [pm] |
|---|---|---|---|---|
| $\mathbf{d\mu(n=1)}$ | -2663.20 | | | |
| $\mathbf{p\mu(n=1)}$ | -2528.49 | | | |
| ... | ... | ... | ... | ... |
| $\mathbf{d\mu(n=2)}$ | -665.80 | | | |
| 0 | -640.77 - 0.5i | 9.8 | 4.1* | 9.4 |
| 0 | -635.31 - 0.2i | 16.4 | 2.8 | 15.6 |
| 0 | -633.31 - 0.1i | 26.5 | 2.4 | 25.7 |
| 0 | -632.57 | 41.7 | 2.1 | 40.9 |
| $\mathbf{p\mu(n=2)}$ | -632.12 | | | |

- 2 bound states + 24 resonant states (mostly newly reported)
- channel composition from $[d\mu(n=2)]$ to $[p\mu(n=2)]$
- The rms radii provide direct evidence for this structural evolution ⇒ $r_{d\mu}^{rms}$ increases and $r_{p\mu}^{rms}$ decreases

# Double-muonic hydrogen molecules

- 4-body systems with bound state or resonant states ($N_{basis} = 5000$, ESVM)

$\mu^-\mu^-p^+p^+$ (L=0)



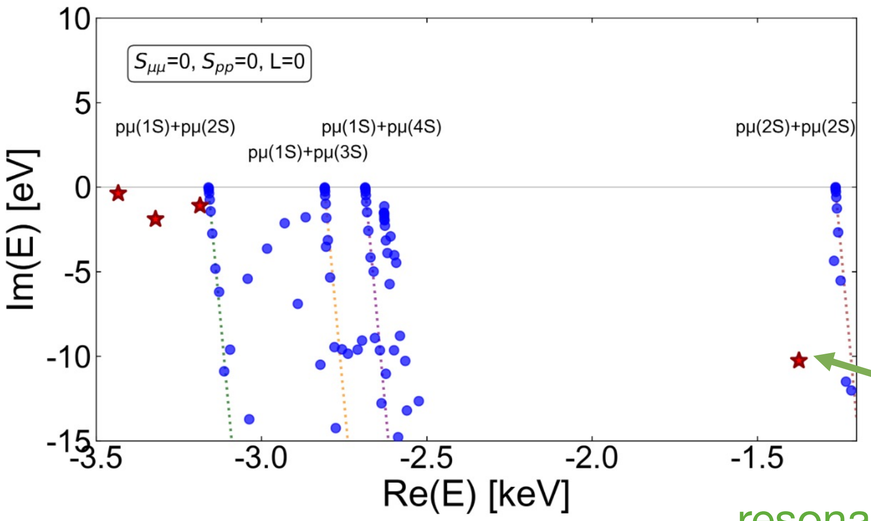

| $[S_{\mu\mu}, S_{pp}, L]$ | $E$ [eV] | Type | $r_{p\mu}^{rms}$ [pm] | $r_{pp}^{rms}$ [pm] | $r_{\mu\mu}^{rms}$ [pm] | $E_{bench}$ [eV] |
|---|---|---|---|---|---|---|
| [0, 0, 0] | -5431.91 | B | 0.62 | 0.64 | 0.81 | -5431.5 [28] |
| $\mathbf{p\mu(n=1)+p\mu(n=1)}$ | -5056.99 | | | | | |
| [0, 0, 0] | -3433.18-0.4i | R | 1.4 | 1.5 | 1.5 | -3370-0.16i [22] |
| [0, 0, 0] | -3321.23-2.5i | R | 1.6 | 1.2 | 2.1 | -3259-4.3i [22] |
| [0, 0, 0] | -3186.55-0.9i | R | 2.0 | 2.6 | 2.1 | |
| [1, 0, 0] | -3430.15 | B | 1.4 | 0.8 | 1.9 | -3406 [22] |
| [0, 1, 0] | -3554.44 | B | 1.1 | 1.2 | 1.2 | -3449 [22] |
| [0, 1, 0] | -3296.14 | B | 1.5 | 1.9 | 1.4 | -3194 [22] |
| $\mathbf{p\mu(n=1)+p\mu(n=2)}$ | -3160.62 | | | | | |
| [0, 0, 0] | -1374.56-10.3i | R | 4.0 | 5.1 | 5.2 | |
| $\mathbf{p\mu(n=2)+p\mu(n=2)}$ | -1264.25 | | | | | |

- 4 bound state + 3 resonances (below n=2 threshold)
- Bound-state energy agrees with GEM (deeper by $\sim 0.4$ eV)
  Hamahata et al., Hyperfine Interact. (2001)
- Two previously reported resonances in the [0,0,0] sector become more deeply bound in our calculation (by $\sim 60$ eV); additional resonances are identified
  Yang et al., PRA (2025)

# Double-muonic hydrogen molecules

- 4-body systems with bound state or resonant states ($N_{basis} = 5000$, ESVM)

$\mu^-\mu^-p^+p^+$ (L=0)



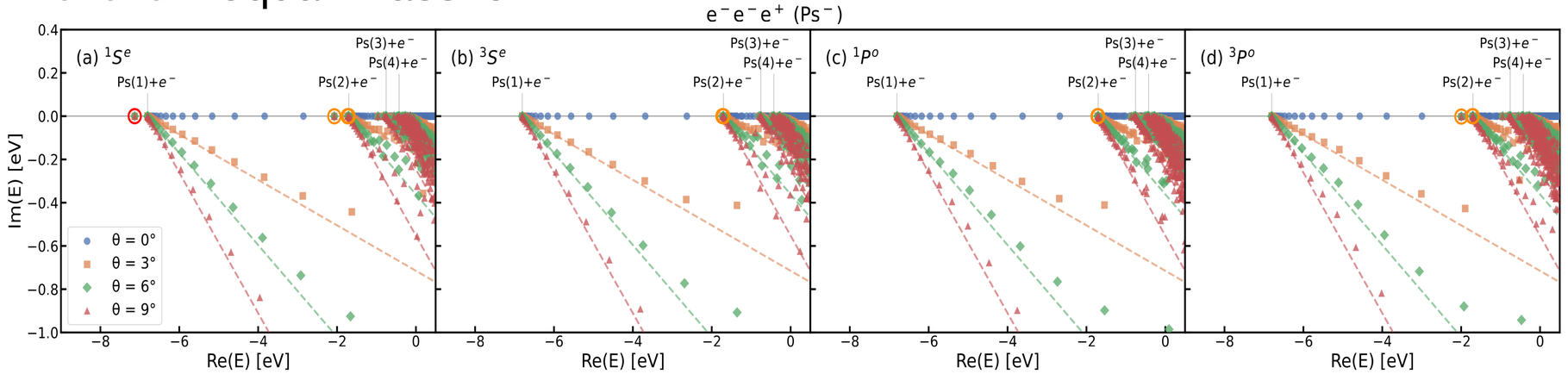

| $[S_{\mu\mu}, S_{pp}, L]$ | $E$ [eV] | Type | $r_{p\mu}^{rms}$ [pm] | $r_{pp}^{rms}$ [pm] | $r_{\mu\mu}^{rms}$ [pm] | $E_{bench}$ [eV] |
|---|---|---|---|---|---|---|
| $[0,0,0]$ | -5431.91 | B | 0.62 | 0.64 | 0.81 | -5431.5 [28] |
| $\mathbf{p\mu(n=1)+p\mu(n=1)}$ | -5056.99 | | | | | |
| $[0,0,0]$ | -3433.18-0.4i | R | 1.4 | 1.5 | 1.5 | -3370-0.16i [22] |
| $[0,0,0]$ | -3321.23-2.5i | R | 1.6 | 1.2 | 2.1 | -3259-4.3i [22] |
| $[0,0,0]$ | -3186.55-0.9i | R | 2.0 | 2.6 | 2.1 | |
| $[1,0,0]$ | -3430.15 | B | 1.4 | 0.8 | 1.9 | -3406 [22] |
| $[0,1,0]$ | -3554.44 | B | 1.1 | 1.2 | 1.2 | -3449 [22] |
| $[0,1,0]$ | -3296.14 | B | 1.5 | 1.9 | 1.4 | -3194 [22] |
| $\mathbf{p\mu(n=1)+p\mu(n=2)}$ | -3160.62 | | | | | |
| $[0,0,0]$ | -1374.56-10.3i | R | 4.0 | 5.1 | 5.2 | |
| $\mathbf{p\mu(n=2)+p\mu(n=2)}$ | -1264.25 | | | | | |

resonant states

ESVM resolves highly excited near-threshold resonances around the $[p\mu(2S) + p\mu(2S)]$ threshold

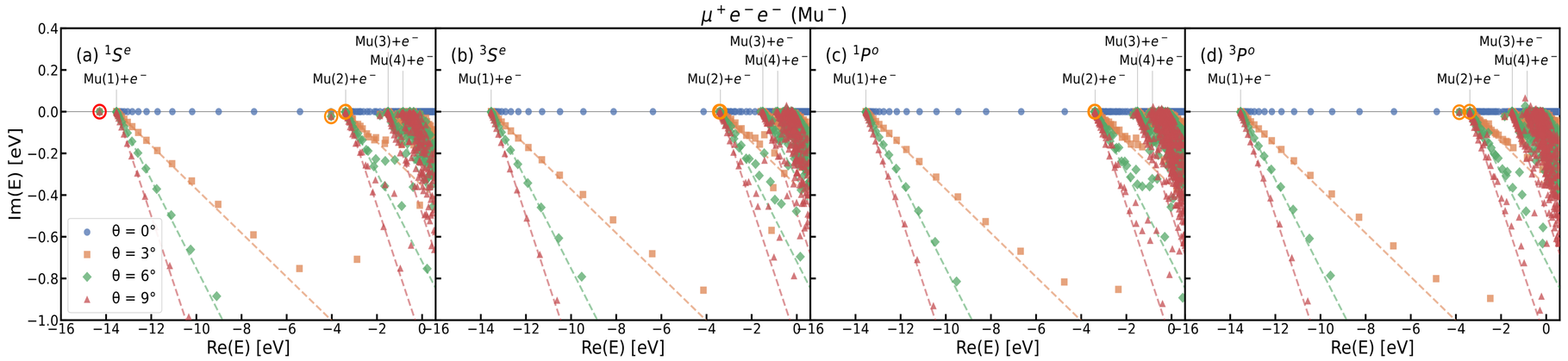
# Trilepton systems

## $e^+e^-e^-$: equal-mass ion




| | $v$ | type | $E$ | $\Gamma/2$ |
|---|---|---|---|---|
| $^1S^e\ (0,0)$ | | | | |
| | 0 | B | −7.1295 | 0 |
| **Ps(1) + $e^-$** | | | **−6.8028** | |
| | 0 | R | −2.0689 | 0.576 |
| | 1 | R | −1.7320 | 0.121 |
| | 2 | R | −1.7032 | 0.151 |
| $^3S^e\ (1,0)$ | | | | |
| | 0 | R | −1.7289 | 0.000 |
| | 1 | R | −1.7027 | 0.262 |
| $^1P^o\ (0,1)$ | | | | |
| | 0 | R | −1.7186 | 0.013 |
| | 1 | R | −1.7015 | 0.097 |
| $^3P^o\ (1,1)$ | | | | |
| | 0 | R | −1.9954 | 1.770 |
| | 1 | R | −1.7170 | 0.226 |
| | 2 | R | −1.7014 | 0.104 |
| **Ps(2) + $e^-$** | | | **−1.7007** | |

## $\mu^+e^-e^-$: atomic ion



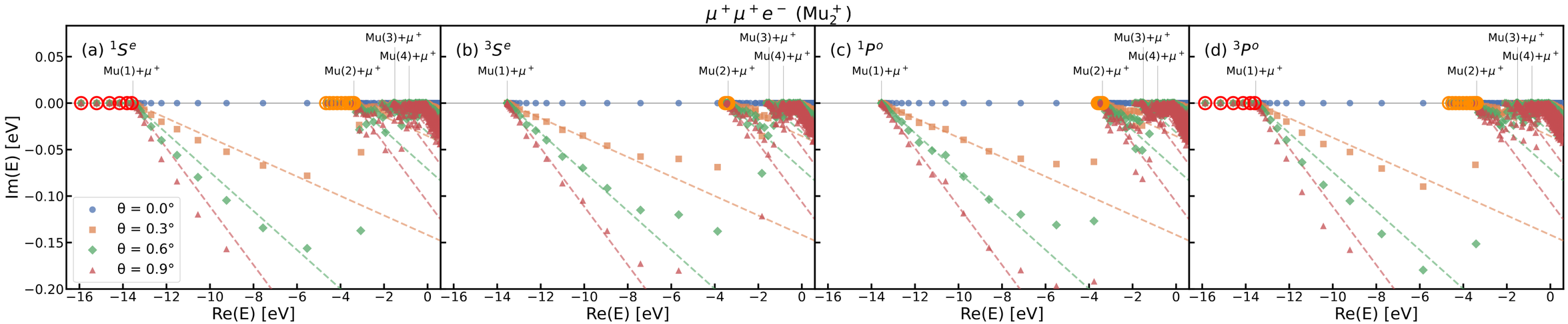

| | | | This work | | Lit. | |
|---|---|---|---|---|---|---|
| | $v$ | type | $E$ | $\Gamma/2$ | $E$ | $\Gamma/2$ |
| $^1S^e\ (0,0)$ | | | | | | |
| | 0 | B | −14.2875 | 0 | −14.2875 [32, 33] | 0 |
| **Mu(1) + $e^-$** | | | **−13.5402** | | | |
| | 0 | R | −4.0291 | 22.695 | −4.0288 [32] | 23.283 |
| | 1 | R | −3.4127 | 1.247 | — | — |
| | 2 | R | −3.3863 | 0.070* | — | — |
| $^3S^e\ (1,0)$ | | | | | | |
| | 0 | R | −3.4419 | 0.009 | — | — |
| | 1 | R | −3.3881 | 0.070* | — | — |
| $^1P^o\ (0,1)$ | | | | | | |
| | 0 | R | −3.4134 | 0.019 | — | — |
| | 1 | R | −3.3856 | 0.105* | — | — |
| $^3P^o\ (1,1)$ | | | | | | |
| | 0 | R | −3.8493 | 2.675 | — | — |
| | 1 | R | −3.3962 | 0.064 | — | — |
| **Mu(2) + $e^-$** | | | **−3.3851** | | | |

Energies are in eV and half-widths $\Gamma/2$ in meV.

- Both systems support shallow resonances below the n=2 threshold

# Trilepton systems

## $\mu^+\mu^+e^-$: molecular ion




- 6 bound states in both $^1S^e$ and $^3P^o$ channel
- Approximate BO S/P pairing
- Below Mu(2)+$\mu^+$: dense Feshbach sequences, including 19 members in $^1S^e$ and 20 in $^3P^o$

# Gailitis–Damburg(GD) dipole sequences

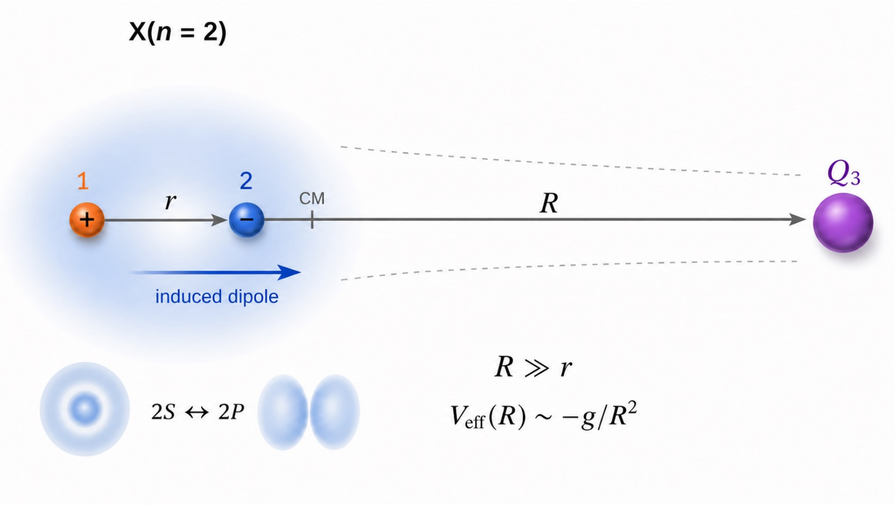
Gailitis & Damburg, PPS (1963); Gailitis, JPB (1982)

## Reduced masses

$$\mu_X = \frac{m_1 m_2}{m_1 + m_2}, \qquad \mu_R = \frac{m_3(m_1 + m_2)}{m_1 + m_2 + m_3}, \qquad \eta = \frac{\mu_R}{\mu_X}.$$

## Dipole coupling at the degenerate $n = 2$ threshold

$$V_{\rm dip} = -\alpha Q_3 \, \frac{\boldsymbol{r}\cdot\boldsymbol{R}}{R^3}.$$




## Large-$R$ coupled Schrödinger equation

$$\sum_j \left[ -\frac{\delta_{ij}}{2\mu_R}\frac{d^2}{dR^2} + \frac{\Lambda_{ij}}{2\mu_R R^2} - \frac{D_{ij}}{R^2} \right] u_j(R) = E\, u_i(R).$$

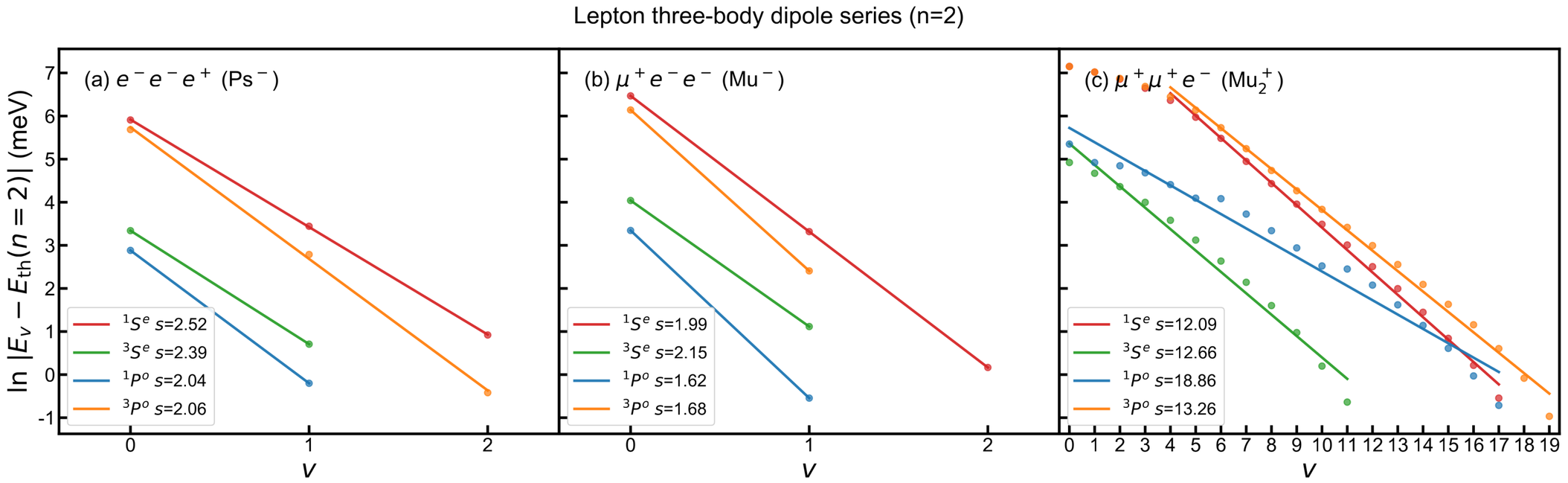
$$\Lambda_{ij} = \lambda_i(\lambda_i + 1)\delta_{ij}, \qquad D_{ij} = \alpha Q_3 \langle 2\ell_i | r | 2\ell_j \rangle A_{ij}.$$

## Supercritical channel and GD scaling

$$V_{\rm eff}(R) = -\frac{g}{R^2}, \qquad x_k > \frac{1}{4}, \qquad s_k = \sqrt{x_k - \frac{1}{4}}, \qquad s = \max_k s_k.$$

$$\frac{|E_{v+1} - E_{\rm th}|}{|E_v - E_{\rm th}|} = e^{-2\pi/s}.$$

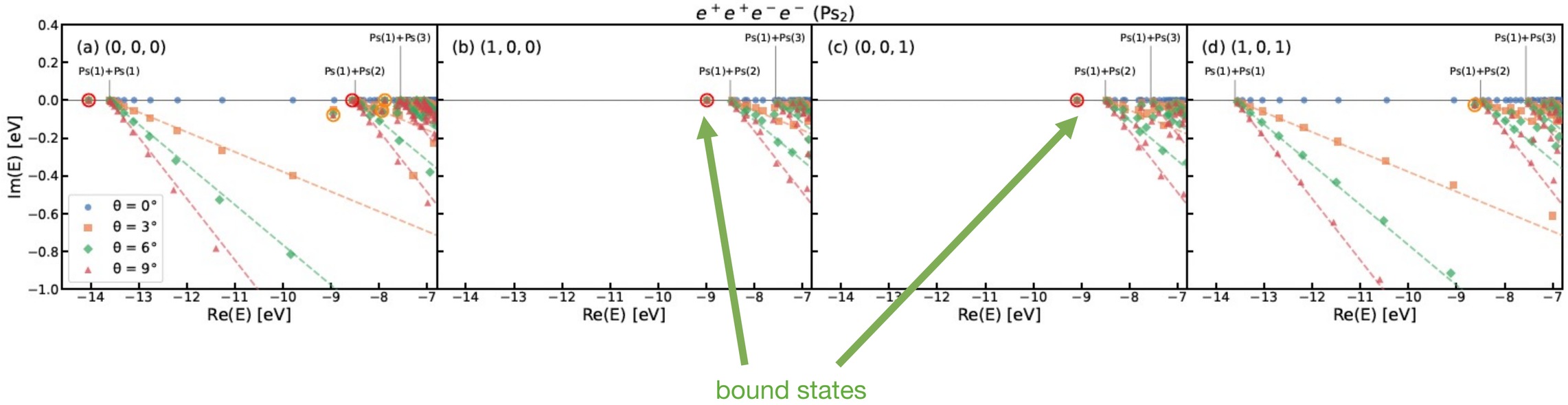
# GD sequences are sparse in $Ps^-$ and $Mu^-$ but dense in $Mu_2^+$




| system | $s$ (dipole limit) | $s$ (fit) | |
|---|---|---|---|
| | | singlet | triplet |
| $Mu^-$ $(L{=}0)$ | 2.20 | 1.99 | 2.15 |
| $Mu^-$ $(L{=}1)$ | 1.86 | 1.62 | 1.68 |
| $Ps^-$ $(L{=}0)$ | 2.61 | 2.52 | 2.39 |
| $Ps^-$ $(L{=}1)$ | 2.30 | 2.04 | 2.06 |
| $Mu_2^+$ $(L{=}0)$ | 24.97 | 12.09 | 12.66 |
| $Mu_2^+$ $(L{=}1)$ | 24.93 | 18.86 | 13.26 |

- $Ps^-$ and $Mu^-$ contain only a few resolvable members
- The heavy spectator in $Mu_2^+$ produces a much denser sequence
- $s_{fit} < s_{dipole}$ in $Mu_2^+$ *indicates finite* $R$, *pre* $-$ *asymptotic corrections*

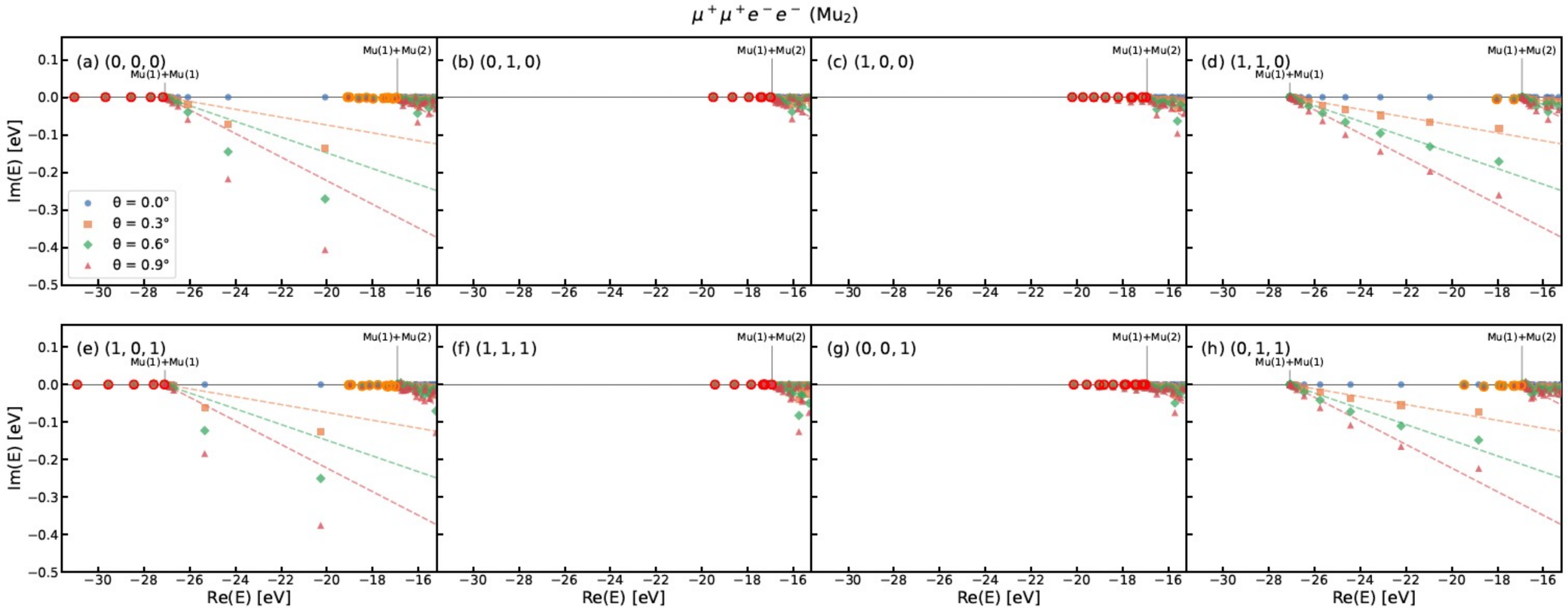
# Tetralepton systems




Exchange symmetry removes the $[e^-e^+\ (1S) + e^-e^+(1S)]$ scattering channel in selected $[S_{e^-e^-}, S_{e^+e^+}, L]$ sectors.

- Pauli-forbidden $Ps(1) + Ps(1)$ channels convert selected states into genuine bound states
- The $(1,0,0)$ bound state appears only when the degenerate $1S + 2S$ and $1S + 2P$ configurations are coupled
  Ma et al., Phys. Rev. D 111, 073001 (2025)
- The $(0,0,1)$ state is the first $L = 1$ bound excitation accessed through the near-251 nm E1 transition
  Cassidy et al., PRL 108, 133402 (2012)

# Tetralepton systems




- Exchange symmetry stabilizes a rich bound-state spectrum: $Mu_2$ supports a rich spectrum of 44 bound levels: 20 S-wave and 24 P-wave states.
- Heavy $\mu^+$motion produces very narrow resonances, as in $Mu_2^+$.

# Summary

**ESVM+CSM**

- Unified bound + resonant-state calculations
- Straightforward extension to higher orbital angular momenta $(L > 0)$

**Muon–nucleus Coulomb systems ($\mu^-\mu^- X^+, \mu^- X^+ X^+, \mu^- X^+ Y^+, \mu^-\mu^- X^+ X^+$)**

- Narrow BO-like resonances in homonuclear molecular ions $\mu^- X^+ X^+$
- channel mixing broadens heteronuclear resonances $\mu^- X^+ Y^+$

**Trilepton systems ($e^- e^- \mu^+, e^- e^- e^+, e^- \mu^+ \mu^+$)**

- Degenerate 2S–2P channels generate Gailitis–Damburg sequences through dipole interaction
- Large mass imbalance produces exceptionally dense S- and P-wave sequences in $Mu_2^+(e^-\mu^+\mu^+)$

**Tetralepton systems ($e^- e^- e^+ e^+, e^- e^- \mu^+ \mu^+$)**

- Exchange symmetry can forbid the lowest dissociation channel and stabilize additional bound states
- mass asymmetry strongly suppresses the widths in $Mu_2$ $(e^- e^- \mu^+ \mu^+)$

Thanks for your attention!




# Thanks for your attention!